THE ASTROPHYSICAL JOURNAL, 290:171–184, 1985 March 1

THE NATURE OF THE LOW-LUMINOSITY GLOBULAR CLUSTER X-RAY SOURCES

PAUL HERTZ[1] AND KENT S. WOOD
E. O. Hulburt Center for Space Research, Naval Research Laboratory
Received 1984 July 25; accepted 1984 September 7

ABSTRACT

An X-ray survey of 134 galactic globular clusters has been conducted with the Large Area Sky Survey Experiment aboard *HEAO 1*. No new globular cluster X-ray sources were discovered, and improved upper limits were obtained on X-ray emission from 67 globular clusters. The lack of new sources confirms the gap in the globular cluster luminosity function noted by Hertz and Grindlay. By combining the *HEAO 1* survey with the *Einstein* globular cluster survey, severe constraints are placed on the existence of any globular cluster X-ray sources with luminosities between $10^{34.5}$ and 10^{36} ergs s^{-1} (0.5–20 keV).

Statistical analyses reveal that the presence of both high- and low-luminosity globular cluster X-ray sources is significantly correlated with the time scale for binary formation via the tidal capture mechanism within globular clusters. This is interpreted as evidence in favor of formation of X-ray binaries in globular clusters via the tidal capture process. A simple analytical calculation has been carried out under the assumption that low-luminosity globular cluster X-ray sources are tidally captured white dwarfs accreting matter from a Roche lobe filling, low-mass companion, as first suggested by Hertz and Grindlay. The calculated luminosity function of low-luminosity globular cluster X-ray sources agrees with that observed in the X-ray surveys. Several predictions, including a turnover in the luminosity function below 10^{32} ergs s^{-1}, are made on the basis of our model calculations. The absence of known cataclysmic variables with X-ray luminosities in excess of 10^{33} ergs s^{-1} is discussed.

Subject headings: clusters: globular — luminosity function — X-rays: binaries — X-rays: sources

I. INTRODUCTION

There are several reasons to search for and study X-ray sources in globular clusters. Since the distances to globular clusters are known from various techniques, the luminosities of globular cluster X-ray sources can be reliably determined. This makes globular cluster X-ray sources unique among low-mass X-ray binaries (LMXRBs), as the distances to very few LMXRBs are accurately known on a source-by-source basis. The study of the stellar dynamics, surface brightness profiles, and color-magnitude diagrams of globular clusters has led to a general understanding of the dynamics in the cluster. This is a second feature which aids in the study of globular cluster X-ray sources.

Hertz and Grindlay (1983*b*, hereafter HG) recently surveyed over half of the known galactic globular clusters with the HRI and IPC imaging detectors aboard the *Einstein Observatory* (Giacconi *et al.* 1979). They determined that the luminosity function for the brightest globular cluster X-ray sources is bimodal with a gap from $\sim 10^{34.5}$ to $\sim 10^{36}$ ergs s^{-1} (0.5–4.5 keV) in which no X-ray sources are found. There are eight sources more luminous than 10^{36} ergs s^{-1}; these are the well-studied luminous globular cluster X-ray sources known prior to the launch of *Einstein*. These eight sources, seven of which have been observed to burst, are LMXRBs and probably consist of a neutron star accreting matter from a Roche lobe filling, low-mass companion (cf. McClintock and Rappaport 1984, and references therein). Hertz and Grindlay (1983*a*) identified the ~ 14 sources fainter than $10^{34.5}$ ergs s^{-1} as accreting white dwarfs for several reasons: (*i*) their X-ray luminosity is $\sim 10^{-3}$ times that of the more luminous sources, consistent with the ratio of gravitational potentials on the surfaces of white dwarfs and neutron stars; (*ii*) their maximum X-ray luminosity is consistent with that predicted by models of accreting white dwarfs (Kylafis and Lamb 1979, 1982); (*iii*) several are located outside of the cluster cores, indicating a low-mass ($\lesssim 0.9\ M_\odot$) system; and (*iv*) the number of sources observed agrees roughly with that expected if the binary systems formed as a result of tidal capture (Fabian, Pringle, and Rees 1975; Press and Teukolsky 1977) of the white dwarf by a globular cluster field star.

In this paper we report an X-ray survey of 134 galactic globular clusters; this represents a complete sample of all of the galactic globular clusters known to us. We have used the Large Area Sky Survey Experiment aboard *HEAO 1* to obtain upper limits $\lesssim 1$ UFU for the X-ray emission from these clusters (§ II); no new globular cluster X-ray sources were detected. We have combined our results with those of HG to construct an improved luminosity function for the brightest globular cluster X-ray sources (§ III) and constrain the bimodal nature of the luminosity function. Correlations of source existence with globular cluster structural and dynamical properties indicate a statistically significant preference for the presence of an X-ray source in a cluster with a short timescale for binary formation via tidal capture (§ IV). In § V we develop a simple model for the formation of low-luminosity globular cluster X-ray sources via tidal capture and show how even a simple model can adequately explain the observed luminosity function. Finally we discuss the implications of our model on the evolution of globular cluster X-ray sources and on LMXRBs and cataclysmic variables (CVs) in the galactic plane (§ VI).

[1] NRC-NRL Cooperative Research Associate.

II. THE *HEAO* A-1 GLOBULAR CLUSTER SURVEY

We have used the NRL Large Area Sky Survey Experiment on the *HEAO 1* satellite, also known as *HEAO* A-1, to conduct our survey. The A-1 experiment consisted of an array of large-aperture proportional counter modules with collimators of varying fields of view (Wood *et al.* 1984). Data from the four $1° \times 4°$ FWHM scan modules have been combined into 4 day summations; these summations allow detection of X-ray sources as faint[2] as $\sim 1.3 \times 10^{-3}$ counts cm^{-2} s^{-1}. Except at high ecliptic latitudes, where sky coverage is more complete, and low galactic latitudes, where source confusion is problematic, this represents the typical limiting sensitivity of the A-1 experiment in scanning mode.

The positions of 134 galactic globular clusters have been searched in the A-1 data base for X-ray emission. Our list of globular clusters is drawn from Madore (1980) with the infrared clusters UKS 1751−241 (Longmore and Hawarden 1980) and Grindlay 1 (Grindlay and Hertz 1981) added. Using the known ephemeris of the *HEAO 1* satellite and the globular cluster positions, we computed the transit time and scan longitude at transit of each cluster during the first 8 months of the *HEAO 1* mission (1977 August–1978 April). A point source was fitted at the scan longitude of each cluster in the 4 day data summation centered (in time) nearest to the cluster's transit time. Scan data $\pm 2°$ from the cluster position were used for estimating the background. Sources which transited twice (once within the first 2 months of the mission and again 6 months later) were fitted during each transit. If no significant flux was detected at the position of a globular cluster, a 3 σ upper limit was derived for X-ray emission from that cluster.

In a survey with a scanning instrument as sensitive as A-1, source confusion becomes a problem. Eight globular clusters transit at the same ($\Delta < 0.^{\circ}2$) scan longitude as a nearby, bright X-ray source. The error boxes for the bright X-ray sources (Wood *et al.* 1984) were checked, and none of them contain the globular cluster in question. Upper limits on the X-ray emission from these eight clusters have been determined using data from the more finely collimated, but less sensitive, $1° \times 0.^{\circ}5$ FWHM module.

Faint (noncataloged) X-ray sources were detected near the positions of several globular clusters. Refinement of the error boxes using 1 day data summations for the $1° \times 4°$ scan modules as well as the $1° \times 0.^{\circ}5$ module usually eliminated the globular cluster from consideration as the counterpart to the X-ray source. In these cases, an upper limit equal to the detected flux of the faint source (or 3 σ, whichever was greater) was tabulated. The error box for the faint source H1825−331 contains the globular cluster NGC 6652. The 90% confidence error box has an area of 2.7 deg^2. Although NGC 6652 cannot be ruled out as the counterpart to H1825−331, it is likely to be a chance superposition of the globular cluster and the X-ray source error box. There are ~ 500 unidentified faint X-ray sources in the 1H catalog (Wood *et al.* 1984). Since the error box for a typical unidentified source is ~ 0.5 deg^2, we expect ~ 0.9 positional coincidences between faint, unidentified X-ray sources and galactic globular clusters. Thus it is not unlikely to find a coincidence such as H1825−331 and NGC 6652; we also note that 2.7 deg^2 in Sagittarius contains an adequate number of optical counterpart candidates. We have tabulated the flux of H1825−331 as the upper limit to X-ray emission from NGC 6652.

All eight of the luminous globular cluster X-ray sources were detected with A-1. These sources were bright enough to detect in 1 day data summations. We have fitted each source's flux in all daily sums for which the collimator response to the source exceeded 0.30 and tabulated the average flux. Most of the luminous sources showed significant variability from day to day; a complete study of the variability of the luminous globular cluster X-ray sources and other LMXRBs will be reported in a later paper. The Rapid Burster (MXB 1730−335 located in the globular cluster Liller 1) was burst-active in the fall of 1977; we have tabulated the average flux during periods of burst activity.

In Table 1 we give the results of our survey. In column (1) is the common name of each cluster, and its 1980 coordinates are given in column (2). Column (3) contains the distance (in kpc) to each cluster; except where noted, these distances are calculated from the distance moduli and color excesses in Table 1 of Madore (1980). The detected X-ray flux, or 3 σ upper limit, is given in columns (4) and (5) in units of 10^{-3} counts cm^{-2} s^{-1} and 10^{-12} ergs cm^{-2} s^{-1} (0.5–20 keV), respectively. Finally we give the X-ray luminosity in columns (6) and (7) (see below for method of calculation) and notes and references in column (8).

In order to estimate the X-ray luminosity from our measurements of the X-ray flux, we have made an approximate correction for interstellar absorption. Using standard relations between visual and X-ray extinction (Gorenstein 1975; Zombeck 1982), and assuming a 5 keV exponential spectrum for a typical globular cluster X-ray source (HG), we find that the fraction of the 0.5–20 keV X-ray flux absorbed is $\sim 0.15 \times {E_{B-V}}^{0.7}$ over the range of interest, where E_{B-V} is the color excess of the globular cluster. Using values of E_{B-V} from Madore (1980), unless otherwise noted, and the distances in Table 1, we have calculated the 0.5–20 keV X-ray luminosities implied by our survey; the common logarithm of the X-ray luminosity in units of ergs s^{-1} is reported in column (6) of Table 1. In column (7) we give the logarithm of the 0.5–20 keV X-ray luminosity from the *Einstein* survey of HG. We have multiplied the *Einstein* luminosities by a correction factor of 1.78 to convert from the 0.5–4.5 keV band of *Einstein* to the 0.5–20 keV *HEAO* A-1 band; this correction factor is appropriate for a 5 keV exponential spectrum.

We detected no new globular cluster X-ray sources. The observed fluxes for the low-luminosity globular cluster X-ray sources (HG) are consistent with our upper limits. All of the previously known luminous X-ray sources were detected by A-1 and the fluxes lie within the range of previous observations. The results of the combined A-1 and *Einstein* surveys are shown in Figure 1. The combined surveys have essentially eliminated the possibility that a bright ($\gtrsim 5 \times 10^{-11}$ ergs cm^{-2} s^{-1}) X-ray source remains undetected in a galactic globular cluster. In Table 2 we give the completeness of the combined survey as a function of limiting flux. This is an order of magnitude improvement over the previous complete survey, the *Uhuru* mission (Ulmer *et al.* 1976; Forman *et al.* 1978).

In Table 3 we show the completeness of the combined survey as a function of limiting luminosity. Note that >90% of galactic globular clusters have been surveyed to a limiting luminosity $< 10^{36}$ ergs s^{-1}, the lowest luminosity observed for a luminous globular cluster X-ray source. Since many of the 13 clusters with limiting luminosities above this value are located at large (≥ 30

[2] 10^{-3} counts cm^{-2} $s^{-1} \approx 8.0 \times 10^{-12}$ ergs cm^{-2} s^{-1} (0.5–20 keV) ≈ 0.2 UFU (2–6 keV).

TABLE 1

HEAO A-1 X-RAY SURVEY OF GALACTIC GLOBULAR CLUSTERS

GLOBULAR CLUSTER (1)	R.A., DECL. (1950) (2)	DISTANCE (kpc) (3)	*HEAO* A-1 FLUX (10^{-3} counts cm^{-2} s^{-1}) (4)	*HEAO* A-1 FLUX (10^{-12} ergs cm^{-2} s^{-1}) (0.5–20 keV) (5)	LOG (L_x) (ergs s^{-1}) (0.5–20 keV) *HEAO* (6)	LOG (L_x) (ergs s^{-1}) (0.5–20 keV) *Einstein* (7)	NOTES (8)
NGC 104	00^h21^m8, −72°21′	4.6	<1.3	<10.4	<34.4	34.5	1
NGC 288	00 50.2, −26 52	8.3	<1.0	<8.3	<34.8	...	
NGC 362	01 01.6, −71 07	9.0	<1.4	<10.9	<35.0	<33.7	2
NGC 1261	03 10.9, −55 25	13.4	<0.9	<7.3	<35.2	<33.8	
Pal 1	03 25.7, +79 28	46.	<0.7	<5.6	<36.2	...	2
AM − 1	03 53.6, −49 45	116.	<0.4	<2.8	<36.7	...	3
Eridanus	04 22.6, −21 18	80.	<1.8	<14.7	<37.1	...	
Pal 2	04 43.1, +31 23	...	<0.8	<6.3	...	...	
NGC 1851	05 12.4, −40 05	10.8	21.5	171.9	36.4	36.5	4, 5
NGC 1904	05 22.2, −24 33	13.3	<1.2	<9.3	<35.3	34.1	
NGC 2298	06 47.2, −35 57	12.2	<0.2	<1.4	<34.4	<33.5	
NGC 2419	07 34.8, +39 00	93.	<1.0	<7.8	<36.9	<35.9	
NGC 2808	09 10.9, −64 39	9.1	<1.6	<12.9	<35.1	<33.6	
Pal 3	10 03.0, +00 18	96.	<1.3	<10.6	<37.1	...	
NGC 3201	10 15.5, −46 09	4.9	<0.9	<7.2	<34.3	...	
Pal 4	11 26.6, +29 16	93.	<2.5	<19.7	<37.3	...	
NGC 4147	12 07.6, +18 49	17.5	<0.9	<7.2	<35.4	...	
NGC 4372	12 23.0, −72 24	4.8	<0.6	<4.9	<34.2	...	
NGC 4590	12 36.8, −26 29	9.6	<2.1	<16.7	<35.3	<33.3	
NGC 4833	12 56.0, −70 36	5.4	<4.1	<33.0	<35.1	<33.1	2
NGC 5024	13 10.5, +18 26	17.2	<1.0	<8.1	<35.5	<33.9	
NGC 5053	13 13.9, +17 57	15.1	<0.9	<7.0	<35.3	...	
NGC 5139	13 23.8, −47 13	5.1	<0.2	<1.5	<33.7	33.7	
NGC 5272	13 39.9, +28 38	9.8	<1.5	<12.0	<35.1	33.8	2
NGC 5286	13 43.0, −51 07	8.8	<1.5	<11.7	<35.1	...	
NGC 5466	14 03.2, +28 46	14.4	<1.9	<15.1	<35.6	...	
NGC 5634	14 27.0, −05 45	22.	<0.7	<5.2	<35.5	<33.9	
NGC 5694	14 36.7, −26 19	32.	<1.6	<12.7	<36.2	<34.5	
IC 4499	14 52.7, −82 02	18.4	<1.3	<10.5	<35.7	...	2
NGC 5824	15 00.9, −32 53	24.	<4.4	35.0	<36.4	34.5	
Pal 5	15 13.5, +00 05	21.	<1.5	<12.1	<35.8	<33.9	2
NGC 5897	15 14.5, −20 50	12.0	<3.5	<28.3	<35.7	...	
NGC 5904	15 16.0, +02 16	7.6	<1.4	<11.5	<34.9	<33.2	
NGC 5927	15 24.4, −50 29	7.2	<0.4	<3.4	<34.4	...	2
NGC 5946	15 31.8, −50 30	9.3	<0.9	<7.4	<34.9	...	
NGC 5986	15 42.8, −37 37	10.0	<0.6	<4.4	<34.8	...	
Pal 14	16 08.8, +15 05	66.	<3.5	<27.6	<37.2	...	2
NGC 6093	16 14.1, −22 52	8.3	<0.8	<6.8	<34.8	<33.7	2
NGC 6101	16 20.0, −72 06	12.2	<0.8	<6.1	<35.0	...	
NGC 6121	16 20.6, −26 24	2.07	<1.0	<8.4	<33.7	...	
NGC 6144	16 24.2, −25 56	8.0	<0.9	<7.5	<34.8	<33.5	
NGC 6139	16 24.3, −38 44	8.7	<1.2	<9.2	<35.0	...	
NGC 6171	16 29.7, −12 57	5.8	<2.1	<17.2	<34.9	<33.1	2
NGC 6205	16 39.9, +36 33	7.2	<0.8	<6.3	<34.6	...	
NGC 6218	16 44.6, −01 52	5.4	<0.8	<6.0	<34.3	<33.0	
NGC 6229	16 45.6, +44 37	31.	<2.7	<21.3	<36.4	<35.0	
NGC 6235	16 50.4, −22 06	10.3	<1.3	<10.7	<35.2	...	
NGC 6254	16 54.5, −04 02	4.3	<1.0	<7.7	<34.3	<32.8	
NGC 6256	16 56.0, −37 00	7.2	<4.7	<37.4	<35.4	...	2, 6
Pal 15	16 57.6, −00 28	...	<1.0	<8.1	...	...	2
NGC 6266	16 58.1, −30 03	5.9	<1.5	<11.9	<34.7	<33.9	7
NGC 6273	16 59.5, −26 12	10.5	<4.8	<38.2	<35.7	...	
NGC 6284	17 01.5, −24 41	10.0	<1.6	<12.6	<35.2	...	
NGC 6287	17 02.1, −22 38	8.8	<5.6	<44.4	<35.6	...	2
NGC 6293	17 07.1, −26 30	7.2	<26.1	<209.0	<36.1	<34.1	
NGC 6304	17 11.4, −29 24	5.2	<1.7	<13.7	<34.7	...	
NGC 6316	17 13.4, −28 05	12.1	<1.8	<14.7	<35.4	...	
NGC 6325	17 15.0, −23 42	6.5	<3.8	<30.6	<35.2	...	2
NGC 6341	17 15.6, +43 11	7.8	<0.6	<4.5	<34.5	...	
NGC 6333	17 16.2, −18 28	6.8	<0.9	<7.6	<34.6	<33.3	
NGC 6342	17 18.2, −19 32	15.0	<3.0	<23.9	<35.8	<33.6	
NGC 6356	17 20.7, −17 46	17.0	<2.9	<23.4	<35.9	<34.8	2
NGC 6355	17 20.9, −26 19	6.6	<1.9	<15.0	<34.9	...	2
NGC 6352	17 21.6, −48 25	5.4	<1.1	<9.0	<34.5	<32.9	2
Terzan 2	17 24.3, −30 46	10.5	32.8	262.3	36.6	36.8	4, 8, 9, 10
NGC 6366	17 25.1, −05 02	3.9	<0.9	<7.5	<34.2	<32.5	
NGC 6362	17 26.6, −67 01	7.1	<1.5	<11.6	<34.9	...	7, 11

TABLE 1—*Continued*

Globular Cluster (1)	R.A., Decl. (1950) (2)	Distance (kpc) (3)	*HEAO* A-1 Flux (10^{-3} counts cm^{-2} s^{-1}) (4)	*HEAO* A-1 Flux (10^{-12} ergs cm^{-2} s^{-1}) (0.5–20 keV) (5)	Log (L_x) (ergs s^{-1}) (0.5–20 keV) *HEAO* (6)	Log (L_x) (ergs s^{-1}) (0.5–20 keV) *Einstein* (7)	Notes (8)
Terzan 4	17 27.4, −31 33	10.0	<22.7	<182.0	<36.4	...	2, 12, 13
HP − 1	17 27.9, −29 57	10.0	<3.9	<31.4	<35.7	...	2, 12, 13
Grindlay 1	17 28.7, −33 48	10.0	272.2	2177.5	37.6	37.1	4, 10, 14, 15
Liller 1	17 30.1, −33 21	10.0	211.7	1693.2	37.4	37.3	9, 10, 16, 17, 18
NGC 6380	17 32.0, −39 02	10.0	<5.9	<46.9	<35.9	...	7, 12, 13, 19
Terzan 1	17 32.6, −30 26	10.0	<13.1	<105.0	<36.2	...	10, 12, 20
NGC 6388	17 32.6, −44 43	14.3	<0.2	<1.9	<34.7	<34.5	2
Ton. 2	17 32.7, −38 31	10.0	<2.9	<23.3	<35.5	...	2, 12, 13
NGC 6402	17 35.0, −03 14	9.9	<0.7	<5.4	<34.8	<33.3	
NGC 6401	17 35.5, −23 53	6.6	<0.9	<7.1	<34.6	...	2
NGC 6397	17 36.8, −53 39	2.19	<0.7	<5.7	<33.5	...	
Pal 6	17 40.6, −26 12	2.70	<18.2	<145.8	<35.2	<32.3	2
NGC 6426	17 42.4, +03 12	15.7	<0.6	<5.0	<35.2	...	
Terzan 5	17 45.0, −24 46	10.0	<5.4	<43.0	<35.8	<34.3	7, 12
NGC 6440	17 45.9, −20 21	3.5	<2.4	<18.8	<34.5	33.1	7
NGC 6441	17 46.8, −37 02	10.1	111.7	893.4	37.0	37.0	4, 5
Terzan 6	17 47.5, −31 16	10.0	<15.9	<127.5	<36.3	...	2, 12, 13
NGC 6453	17 48.0, −34 37	6.9	<7.4	<59.5	<35.6	...	2
UKS 1751	17 51.4, −24 08	10.0	<17.9	<142.9	<36.4	<33.9	9, 21
NGC 6496	17 55.5, −44 14	9.0	<5.8	<46.4	<35.7	...	2
Terzan 9	17 58.7, −26 52	10.0	<24.7	<197.7	<36.5	...	2, 12, 20
NGC 6517	17 59.1, −08 57	7.4	<1.4	<11.0	<34.9	<33.1	
NGC 6522	18 00.4, −30 02	6.3	<8.8	<70.5	<35.6	<33.1	2
NGC 6535	18 01.3, −00 18	10.8	<1.3	<10.7	<35.2	...	
NGC 6528	18 01.6, −30 04	7.1	<6.2	<49.5	<35.5	<33.3	2
NGC 6539	18 02.1, −07 35	2.16	<0.7	<6.0	<33.6	<32.2	
NGC 6544	18 04.3, −25 01	4.5	<4.5	<36.2	<35.0	...	7, 19
NGC 6541	18 04.4, −43 44	6.8	<0.9	<7.0	<34.6	33.6	2
NGC 6553	18 06.3, −25 56	6.0	<17.5	<140.3	<35.8	...	2
NGC 6558	18 07.0, −31 47	9.0	<10.8	<86.5	<36.0	...	2
IC 1276	18 08.0, −07 14	12.4	<1.7	<13.9	<35.5	...	
Terzan 12	18 09.6, −22 46	10.0	<8.8	<70.7	<36.1	<34.4	12, 20
NGC 6569	18 10.4, −31 50	7.6	<15.0	<119.8	<36.0	<33.3	2
NGC 6584	18 14.6, −52 14	14.5	<1.6	<12.8	<35.5	...	
NGC 6624	18 20.5, −30 23	8.4	844.5	6755.8	37.8	37.9	4, 15
NGC 6626	18 21.5, −24 53	6.0	<5.6	<45.0	<35.3	<34.6	7
NGC 6638	18 27.9, −25 32	7.8	<1.8	<14.5	<35.1	...	
NGC 6637	18 28.1, −32 23	10.2	<0.8	<6.3	<34.9	...	2
NGC 6642	18 28.8, −23 30	6.1	<1.0	<7.7	<34.6	<32.8	
NGC 6652	18 32.5, −33 02	14.9	<1.9	<15.4	<35.6	...	22
NGC 6656	18 33.3, −23 58	3.0	<1.0	<8.0	<34.0	33.0	
Pal 8	18 38.5, −19 52	30.	<1.1	<8.6	<36.0	...	
NGC 6681	18 40.0, −32 21	10.8	<1.6	<12.4	<35.2	<34.0	
NGC 6712	18 50.3, −08 47	7.4	11.8	94.2	35.8	36.3	5, 23
NGC 6715	18 51.9, −30 32	21.	<1.0	<7.7	<35.6	<34.1	2
NGC 6717	18 52.1, −22 47	15.5	<0.8	<6.4	<35.3	<34.5	
NGC 6723	18 56.2, −36 42	8.7	<0.9	<6.9	<34.8	<33.1	
NGC 6749	19 02.5, +01 42	5.0	<5.0	<40.2	<35.1	<32.8	7, 24
NGC 6752	19 06.4, −60 04	4.2	<0.9	<7.5	<34.2	...	2
NGC 6760	19 08.6, +00 57	3.8	<0.9	<7.2	<34.2	...	2
Terzan 7	19 14.4, −34 45	10.0	<1.0	<8.1	<35.0	<33.4	12
NGC 6779	19 14.6, +30 05	9.4	<1.1	<8.6	<35.0	...	
Pal 10	19 16.0, +18 28	8.5	<1.2	<9.2	<35.0	<33.5	
Arp 2	19 25.6, −30 27	...	<1.1	<8.4	...	...	
NGC 6809	19 36.9, −31 03	6.8	<0.8	<6.6	<34.6	<32.8	
Pal 11	19 42.6, −08 09	11.2	<1.0	<8.2	<35.1	...	
NGC 6838	19 51.5, +18 39	3.9	<1.3	<10.2	<34.3	<32.5	
NGC 6864	20 03.2, −22 04	18.1	<0.5	<3.8	<35.2	<34.7	
NGC 6934	20 31.7, +07 14	14.6	<1.2	<9.6	<35.4	<33.7	
NGC 6981	20 50.7, −12 44	17.3	<1.0	<8.0	<35.5	<34.0	
NGC 7006	20 59.1, +16 00	35.	<1.1	<8.5	<36.1	<34.5	
NGC 7078	21 27.6, +11 57	9.4	16.7	133.5	36.2	36.5	4, 5
NGC 7089	21 30.9, −01 03	11.2	<1.0	<8.2	<35.1	<33.5	
NGC 7099	21 37.5, −23 25	8.2	<0.9	<7.2	<34.8	<33.2	
Pal 12	21 47.3, −21 28	19.0	<1.0	<7.8	<35.5	...	
Pal 13	23 04.2, +12 28	24.	<0.5	<4.3	<35.5	...	
NGC 7492	23 05.7, −15 54	22.	<1.2	<9.5	<35.7	...	

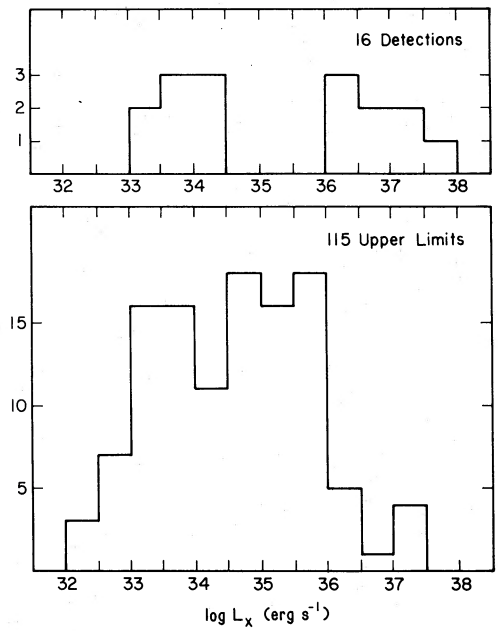

FIG. 1.—Histograms of the results of the combined *HEAO 1* and *Einstein* X-ray surveys of galactic globular clusters. The clusters are plotted as a function of the logarithm of their 0.5–20 keV X-ray luminosity in ergs s^{-1}. (*upper*) Histogram of the 16 globular clusters with observed X-ray emission. The brightest source is plotted for those clusters with resolved multiple sources (i.e., NGC 5139 and NGC 6656; see HG). (*lower*) Histogram of the upper limit to X-ray emission from 115 galactic globular clusters with known distances.

kpc) distances, and since seven of the eight known luminous sources are in the galactic bulge (see § IV), it is likely that there are no undiscovered luminous X-ray sources in the known galactic globular clusters. The results of an infrared survey for obscured globular clusters associated with high-luminosity galactic bulge X-ray sources (Hertz and Grindlay 1984*b*) make it unlikely that there are any undiscovered globular clusters associated with luminous X-ray sources. We thus conclude that the total number of luminous ($> 10^{36}$ ergs s^{-1}) globular cluster X-ray sources in the Galaxy is approximately eight.

III. THE GLOBULAR CLUSTER X-RAY LUMINOSITY FUNCTION

In Figure 1 we presented a summary of the distribution for the X-ray luminosity detections and upper limits of the 131 galactic globular clusters in our survey[3] for which we have a distance estimate. In order to use all of the information available in constructing a luminosity function, we have utilized the DB (detections and bounds) maximum likelihood technique of Avni *et al.* (1980). Our method parallels that of HG; however, our results differ in that we have better constraints on the 60 globular clusters which were not observed with *Einstein*. In addition, our studies are conducted in a slightly broader energy band (0.5–20 keV instead of 0.5–4.5 keV), and thus our luminosities are larger for an assumed 5 keV spectrum.

For each globular cluster, we have determined a single luminosity or upper limit to the luminosity (see Table 1). This luminosity (or luminosity limit) is for the total X-ray luminosity of the globular cluster. We assume that the X-ray emission is due, primarily, to point sources within the globular cluster. In several large, nearby globular clusters, diffuse X-ray emission was detected at a low level with the *Einstein Observatory* (Hartwick, Cowley, and Grindlay 1982). The diffuse emission is lower in luminosity than most detected sources ($L_x < 10^{33.5}$ ergs s^{-1}) and contains $\sim 20\%$–50% of the luminosity that is found in unresolved point sources in the same clusters. We thus are justified in interpreting the luminosities in our survey as the total luminosity from point sources in the cluster.

The bright end of the luminosity function for globular cluster X-ray sources is steep (HG; see § V); therefore, the total luminosity of the cluster is approximately the luminosity of the brightest source. In any case, even if the second brightest source were nearly as bright as the brightest source, the wide luminosity bins (factor of 3) in our histogram would ensure that the bin in which the cluster

[3] Hereafter "survey" refers to the *HEAO* A-1 and *Einstein* combined survey; also all X-ray fluxes and luminosities are in the 0.5–20 keV *HEAO* A-1 band.

NOTES—(1) *Einstein* luminosity from average of IPC and HRI detections; source is apparently variable. (2) Globular cluster within $\pm 1.^{\circ}0$ scan longitude (ecliptic latitude) of a detected X-ray source; the error box of the nearby X-ray source excludes the globular cluster. (3) Reddening and distance from Aaronson, Schommer, and Olszewski 1984. (4) *HEAO 1* flux from average of daily sums of data; source is variable from day to day. (5) *Einstein* luminosity from average of MPC data; source is variable in MPC. (6) Reddening estimated from cosecant reddening law. (7) Globular cluster within $\pm 0.^{\circ}2$ scan longitude (ecliptic latitude) of a detected X-ray source; the X-ray upper limit has been derived from the finely collimated module rather than the scan modules. (8) Distance from Marshall 1982. (9) Reddening from Malkan, Kleinmann, and Apt 1980. (10) Region is source confused in A-1 scan modules. (11) X-ray upper limit from *Uhuru* data; Ulmer *et al.* 1976. (12) Distance assumed to be 10 kpc toward galactic bulge. (13) Reddening assumed to be $E_{B-V} = 1.75$ toward galactic bulge. (14) Reddening and distance from Grindlay and Hertz 1981. (15) *Einstein* luminosity from MPC data. (16) *HEAO 1* flux for average of bursts in daily sums of data; average is variable from day to day. (17) Distance from Kleimann, Kleinmann, and Wright 1976. (18) *Einstein* luminosity from average of bursts in MPC data. (19) X-ray upper limit from *Uhuru* data; Forman *et al.* 1978. (20) Reddening from Huchra and Aaronson 1980. (21) Distance from Malkan, Kleinmann, and Apt 1980. (22) Error box for X-ray source H1825 − 331 includes globular cluster; see text. (23) *HEAO 1* flux from average of daily sums of data. (24) Distance from Kukarkin 1974.

TABLE 2

COMPLETENESS OF GLOBULAR CLUSTER SURVEY AS A FUNCTION OF LIMITING X-RAY FLUX

FLUX LIMIT[a]			A-1 ONLY		A-1 AND *Einstein*	
(10^{-3} A-1 counts cm^{-2} s^{-1})	(10^{-12} ergs cm^{-2} s^{-1}) (0.5–20 keV)	UFU (2–6 keV)	Number	Fraction	Number	Fraction
10.	80.	2.	124	0.93	128	0.96
5.	40.	1.	114	0.85	124	0.93
2.5	20.	0.5	101	0.75	116	0.87
1.0	8.	0.2	52	0.39	89	0.66

[a] Or detection.

TABLE 3

COMPLETENESS OF GLOBULAR CLUSTER SURVEY AS A FUNCTION OF LIMITING X-RAY LUMINOSITY

LOG (luminosity limit)[a] (ergs s^{-1})(0.5–20 keV)	A-1 ONLY		A-1 AND *Einstein*	
	Number	Fraction	Number	Fraction
36.0	113	0.86	121	0.92
35.5	88	0.67	103	0.79
35.0	55	0.42	87	0.66
34.5	24	0.18	69	0.53
34.0	13	0.10	58	0.44
33.5	...	...	42	0.32
33.0	...	...	26	0.20

[a] Or detection.

falls is the same for either the total cluster luminosity or the luminosity of the brightest source. Thus the luminosity function derived from the total cluster luminosity is the same as the brightest source luminosity function (BSLF). HG also derived the BSLF but did not clearly state the difference between it and the traditional luminosity function.

The maximum likelihood BSLF is presented in Figure 2 and summarized in Table 4. We confirm the existence of several features in this function noted by HG. The most obvious feature is the 1.5 orders of magnitude gap in the BSLF between the luminous sources ($>10^{36}$ ergs s^{-1}) and the low-luminosity sources ($<10^{34.5}$ ergs s^{-1}). Using the known statistics of maximum likelihood calculations (see Avni *et al.* 1980 for details), we can determine the probability that any globular cluster contains an X-ray source whose luminosity falls in the gap. The 90% upper limit is 0.004 sources per cluster, or <0.5 sources in the entire Galaxy. It is therefore unlikely that there are any globular cluster X-ray sources in the Galaxy with luminosities falling in the gap of the maximum likelihood BSLF.

Another quantifiable feature of the BSLF is its slope below $10^{34.5}$ ergs s^{-1}, and we have fitted a power law between $10^{33.5}$ and $10^{34.5}$ ergs s^{-1} to determine the slope. The best fitted value is -1.4 ± 0.7 (90% confidence limits). Since the BSLF is normalized (i.e., each cluster has only one brightest source), the function must turn over below our observational threshold. Extrapolating the steep slope to lower luminosities requires the function to turn over near 10^{32} ergs s^{-1}. Thus a typical cluster is expected to have at least one X-ray source brighter than $\sim 10^{32}$ ergs s^{-1}.

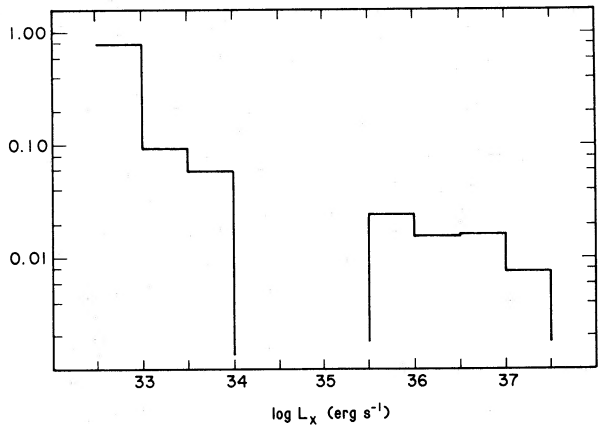

FIG. 2.—The maximum likelihood solution for the brightest source luminosity function (BSLF). The function is normalized to have unit area. Note that the lowest bin contains all luminosities below 10^{33} ergs s^{-1}. The X-ray luminosity is in the 0.5–20 keV band of *HEAO* A-1.

TABLE 4

MAXIMUM LIKELIHOOD BRIGHTEST SOURCE LUMINOSITY FUNCTION (BSLF)

Log (L_x) (ergs s^{-1}) (0.5–20 keV)	Number of Clusters		Probability per Cluster	
	Detections	Upper Limits	Observed	Model[a]
>38.0	0	0	0.000	...
37.5–38.0	1	0	0.008	...
37.0–37.5	2	4	0.016	...
36.5–37.0	2	1	0.016	...
36.0–36.5	3	5	0.025	...
35.5–36.0	0	18	0.000	...
35.0–35.5	0	16	0.000	...
34.5–35.0	0	18	0.000	0.000
34.0–34.5	3	11	0.059	0.027
33.5–34.0	3	16	0.094	0.225
<33.5	2	26	0.784	0.680

[a] See § V; model has been renormalized to match total probability for low-luminosity sources only.

In § V we will use a simple model for the formation of globular cluster X-ray sources to predict the luminosity function. From the luminosity function we derive the associated BSLF. The predicted BSLF matches the observed function well; the luminosity function also predicts a turnover in the number of low-luminosity X-ray sources below $\sim 10^{32.0}$ ergs s^{-1} as well as constraining the number of CVs in globular clusters. However we first discuss which globular clusters are likely to contain X-ray sources.

IV. PROPERTIES OF X-RAY GLOBULAR CLUSTERS

We are interested in determining what, if any, physical properties of globular clusters are correlated with the presence of X-ray sources. Presumably such a correlation provides insight into the formation and evolution of globular cluster X-ray sources. If we assume that the low-luminosity sources form in the same clusters as the high-luminosity sources, either because they form via the same mechanism or because one evolves from the other, then we are interested in determining if any cluster properties are correlated with the presence of both high and low luminosity sources.

The BSLF (Fig. 2) indicates that most, if not all, globular clusters may contain faint X-ray sources. However, those clusters with the most X-ray sources are likely to have the brightest sources; the brightest sources are the only ones detected in the survey. Thus a property correlated with the presence of the brightest X-ray sources is also correlated with a propensity for a cluster to have many X-ray sources.

Many properties of globular clusters have been suggested as being associated with the presence of bright X-ray sources. The bright sources are thought to occur preferentially in highly concentrated globular clusters, and evidence for a correlation with high escape velocities and short relaxation times was noted by Bahcall and Ostriker (1975) soon after the discovery of globular cluster X-ray sources. Recently Lightman and Grindlay (1982) have correlated galactocentric distance and the time scale for binary formation via tidal capture with the presence of bright sources. Attempts at correlating other properties of globular clusters, including optical magnitude (Ulmer *et al.* 1976) and metallicity (Silk and Arons 1975), with the presence of bright sources have also been made.

We have looked for correlations with several cluster parameters which are available for most clusters and, in our opinion, may reasonably be expected to affect the formation and evolution of X-ray sources. These are the cluster's concentration parameter, physical core radius, central density, escape velocity, relaxation time scale, tidal capture time scale, and galactocentric distance. We have used the Kolmogorov-Smirnov test, as discussed by Lightman and Grindlay (1982), to test the data for significant correlations. In this test, the clusters are ordered by the parameter being tested; the distribution of globular clusters containing X-ray sources is then tested to see if it is consistent with having been drawn randomly from the entire sample of clusters. In order to avoid selection effects associated with the variable threshold for X-ray detection in our survey, we have considered only those clusters in which a high- (or low-) luminosity X-ray source could have been (or was) detected. For correlations with the presence of high-luminosity sources, we require that the cluster has been surveyed to 10^{36} ergs s^{-1} to be included; for low-luminosity sources, we require a threshold $< 10^{34.5}$ ergs s^{-1}. We have assumed that the clusters containing luminous sources (with the exception of the diffuse cluster NGC 6712) have not been surveyed adequately to have detected a low-luminosity source.

We have correlated all the clusters which met the luminosity threshold criteria and for which we could obtain data on the parameter in question. However, two of the clusters containing luminous sources were discovered as a result of their X-ray emission, i.e., they are X-ray selected. These are Liller 1 (Liller 1977) and Grindlay 1 (Grindlay and Hertz 1981). In order to eliminate any selection effect which this may introduce, we have also performed the correlations without these clusters. In addition, the distances to several clusters have not been measured but are assumed to be ~ 10 kpc based on their galactocentric location. For cluster properties which depend on the distance (e.g., physical core radius and galactocentric distance), we have also performed the correlations without these clusters. We feel that these correlations are less likely to be biased and thus provide the most reliable basis for drawing conclusions.

We have taken the globular cluster data from several sources. The data on R (galactocentric distance), t_2 (time scale for binary formation via tidal capture), and t_r (relaxation time scale) are from Lightman and Grindlay (1982); the remainder of the structural

TABLE 5

CORRELATIONS OF GLOBULAR CLUSTER PARAMETERS WITH THE PRESENCE OF X-RAY SOURCES

Parameter	Number of Clusters	Number of X-ray Sources	K-S Statistic	Probability	Note
Luminous X-Ray Sources (117 clusters searched to $L_x < 10^{36}$ ergs s^{-1})					
c	86	5	0.319	0.59	
r_c	98	7	0.684	0.001	1, 2
	95	5	0.642	0.016	3, 4
ρ_0	67	3	0.488	0.36	
v_e	38	2	0.868	0.035	
t_r	81	7	0.474	0.057	1
	80	6	0.458	0.11	3
t_2	81	7	0.467	0.064	1
	80	6	0.429	0.16	3
R	117	8	0.522	0.015	1, 2
	108	5	0.363	0.42	3, 4
Low-Luminosity X-Ray Sources (66 clusters searched to $L_x < 10^{34.5}$ ergs s^{-1})					
c	53	7	0.458	0.073	
r_c	60	8	0.200	0.85	4, 5
ρ_0	45	7	0.333	0.34	
v_e	28	7	0.500	0.038	
t_r	53	8	0.198	0.86	5
t_2	53	8	0.403	0.11	5
R	66	8	0.239	0.67	2, 5
	64	8	0.234	0.69	4, 5

NOTES.—(1) X-ray selected clusters included in this correlation. (2) Clusters with assumed (D = 10 kpc) distances included in this correlation. (3) No X-ray selected clusters included in this correlation. (4) No clusters with assumed distances included in this correlation. (5) No X-ray selected clusters were searched for low-luminosity sources.

and dynamic parameters, c (concentration parameter), r_c (core radius), v_e (escape velocity), and ρ_0 (central density), are taken from the compilation of Madore (1980). The core radii of the globular clusters containing luminous sources are from Hertz and Grindlay (1984*c*) and the distances are as referenced in Table 1. In Table 5 we present the results for correlations of globular cluster properties with the presence of X-ray sources. Our threshold criterion for detection of luminous sources was met by 117 clusters, and 66 were tested for correlation with the presence of low-luminosity sources. This number, however, is reduced by the availability of data on each property considered. This introduces some (unquantifiable) selection effects in that poorly studied globular clusters are not included in the correlations.

In Table 5 we give, for the correlation with each parameter, the number of clusters for which data was available, the value of the K-S statistic, and the probability that this value of the statistic could occur by chance. Thus the probability reported is the probability that the X-ray clusters have typical values of the cluster property in question. A low probability indicates a significant correlation. Note that we have used the correct two-tailed K-S test (see the Appendix) rather than the one-tailed test used by Lightman and Grindlay (1982). We find that several globular cluster properties are correlated with the presence of X-ray sources. If we adopt an 80% confidence limit (i.e., look for correlations with chance probabilities <0.20), then we note that two parameters are correlated with the presence of both high- and low-luminosity sources: v_e (escape velocity) and t_2 (tidal capture time scale). Several other properties are significantly correlated with the presence of either high- or low-luminosity sources, but not both. We are not surprised that more than one globular cluster parameter is correlated with the presence of X-ray sources, as most globular cluster properties are strongly correlated with each other. We have cross-correlated the globular cluster properties considered here using a Spearman's rank correlation test (see, e.g., Hays 1973). In Table 6 we show the results of these correlations; the upper half of the

TABLE 6

CROSS CORRELATIONS OF GLOBULAR CLUSTER PARAMETERS[a]

Parameter	c	r_c	ρ_0	v_e	t_r	t_2	R
c	...	92	68	41	76	76	92
r_c	<0.001	...	71	41	83	83	104
ρ_0	<0.001	<0.001	...	41	69	69	71
v_e	<0.001	<0.001	<0.001	...	40	40	41
t_r	0.002	<0.001	<0.001	<0.001	...	84	84
t_2	<0.001	<0.001	<0.001	<0.001	<0.001	...	84
R	0.51	<0.001	0.001	0.018	<0.001	0.002	...

[a] Upper right half of table is number of clusters cross-correlated; lower left half of table is probability of correlation by chance.

table gives the number of clusters whose properties were correlated, and the lower half shows the probability that the properties are uncorrelated. Note that virtually every pair of properties is significantly correlated. This feature had been previously recognized for several pairs of properties (e.g., Ulmer *et al.* 1976; Lightman and Grindlay 1982) and is easily understood since globular cluster structure is described by a three-parameter King (1966) model. Thus a single property (e.g., t_2) correlated with the presence of X-ray sources can easily account for several other properties being correlated.

The correlations indicate that X-ray sources are preferentially found in clusters with short tidal capture time scales. Although this had previously been noted for luminous X-ray sources (Lightman and Grindlay 1982), we have found that it also holds for the low-luminosity sources. This correlation supports the model that globular cluster X-ray sources, both high and low luminosity, form by tidal capture. Clusters with short tidal capture time scales tend to be highly concentrated and to have high escape velocities, high central densities, high central velocity dispersions, short relaxation times, and small core radii; this explains the correlation of these properties with the presence of X-ray sources. We are aware, however, that other models for the formation of globular cluster X-ray sources requiring conditions correlated with short tidal capture times scales may also be supported by these data.

Nevertheless we favor the picture of globular cluster X-ray sources forming by the tidal capture of a compact object (either a white dwarf or a neutron star) by a normal cluster star, as first suggested by Fabian, Pringle, and Rees (1975). Several other pieces of observational and theoretical evidence lend credence to the low-mass binary nature of globular cluster X-ray sources. These include the success of the thermonuclear flash model in explaining the bursters found in globular clusters (Lewin and Joss 1984) and the statistical determination of the low-mass nature of globular cluster X-ray sources (Grindlay *et al.* 1984; Hertz and Grindlay 1983*a*). We show in § V that simple models of tidal capture can correctly predict the major features of the observed globular cluster brightest X-ray source luminosity function.

V. MODELING THE LUMINOSITY FUNCTION

We assume that globular cluster X-ray sources form via the tidal capture mechanism. Our intent in this section is to show that simple assumptions concerning the structure of globular clusters allow us to calculate luminosity functions and BSLFs that reproduce all of the major features of the observed BSLF. Since our assumptions are simple, the resulting luminosity function is insensitive to the exact form of these assumptions. We have made little attempt to optimize the input parameters in order to best fit the luminosity function, as there are more parameters than constraints in the problem. We have used best estimates for all parameters from the current literature. However, we feel that the ability to predict the observed BSLF from simple assumptions provides strong evidence for the validity of the tidal capture mechanism for the formation of globular cluster X-ray sources as well as for the accreting white dwarf nature of the low luminosity sources.

The probability that a stellar member of a globular cluster (or elsewhere, for that matter) with mass between m_s and $m_s + dm_s$ will capture a compact star (in particular a white dwarf) with mass between m_x and $m_x + dm_x$, and will subsequently form an accreting binary with total accretion rate between $\dot{M}$ and $\dot{M} + d\dot{M}$, can be written

$$p(m_s, m_x, \dot{M})dm_s\, dm_x\, d\dot{M} = \Gamma(m_s, m_x) f_s(m_s) f_x(m_x) \phi(\dot{M}) dm_s\, dm_x\, d\dot{M} , \tag{1}$$

where $\Gamma(m_s, m_x)$ is the capture rate for a star of mass m_s to tidally capture a compact object of mass m_x, $f_s(m_s)$ and $f_x(m_x)$ are the mass functions for stars and compact objects in the globular cluster, and $\phi(\dot{M})$ is the distribution function for accretion rates found in Roche lobe overflow systems such as LMXRBs and CVs. We discuss each of these input functions in turn.

Press and Teukolsky (1977) have solved the general problem of two-body tidal capture. To treat the case at hand, we have assumed that no energy is deposited in tidal oscillations of the white dwarf. With this assumption, it is straightforward but tedious to show that equations (51)–(55) of Press and Teukolsky imply

$$\Gamma(m_s, m_x) = 7.1 \times 10^{-16} \left(\frac{n_s}{10^4\ \mathrm{pc}^{-3}}\right)\left(\frac{n_x}{10^4\ \mathrm{pc}^{-3}}\right)\left(\frac{V}{\mathrm{pc}^3}\right)\left(\frac{v_0}{10\ \mathrm{km\ s}^{-1}}\right)^{-1.2}\left(\frac{R_s}{R_\odot}\right)^{0.9}\left(\frac{m_s}{M_\odot}\right)^{-0.3}\left(\frac{m_x}{M_\odot}\right)^{0.1}\left(\frac{m_s + m_x}{M_\odot}\right)^{1.3} \mathrm{s}^{-1} . \tag{2}$$

Here n_s and n_x are the number densities of field stars and white dwarfs, v_0 is the rms velocity dispersion, R_s is the radius of the capturing star, and V is the volume in which the capturing takes place (and in which n_s, n_x, and v_0 are valid). This equation may be compared directly to equation (59) of Press and Teukolsky.

Equation (2) specifies a simply derived form for Γ in which we have assumed constant densities over, say, the core of the cluster and a single velocity dispersion. We have also carried through calculations taking the isothermal nature of the globular cluster into account. Since globular clusters are thermally relaxed (Lightman and Shapiro 1978), more massive stars tend to sink to the center of the cluster and thus have higher densities. In addition, equipartion of energy implies that massive stars have smaller velocity dispersions. When these effects are taken into account, the final luminosity function is within a few percent of that obtained using equation (2). We thus feel justified in using the simplistic form of equation (2) and in concluding that the results of our model calculations are insensitive to the exact form of the capture cross section Γ.

For the mass functions, we have taken simple models from previous studies. The mass function for globular cluster stars is

$$f_s(m_s)dm_s = k_s m_s^{-3} dm_s \tag{3}$$

for $0.3 < (m_s/M_\odot) < 0.8$ (Gunn and Griffin 1979), where k_s is a normalizing constant for the distribution function. The white dwarf mass function is sharply peaked with a mean of $0.6\ M_\odot$ and an rms dispersion of $0.15\ M_\odot$ (Koester and Wiedmann 1980). We have used a Gaussian form for $f_x(m_x)$ with the appropriate parameters in our final calculations; however, a truncated Gaussian (from 0.35 to $0.85\ M_\odot$) gives qualitatively similar results.

Next we specify the distribution of accretion rates, $\phi(\dot{M})$. Several processes have been proposed as powering the accretion in LMXRBs and CVs, including magnetic braking (Rappaport, Verbunt, and Joss 1983; Patterson 1984), gravitational radiation

(Paczyński and Sienkiewicz 1981; Rappaport, Joss, and Webbink 1982), and nuclear evolution of the secondary (Webbink, Rappaport, and Savonije 1983). No single mechanism has been identified as primarily responsible for the evolution of accreting binaries, although much of the recent evidence, both observational and theoretical, points to magnetic braking (cf. Patterson 1984). In lieu of a theoretical model to predict $\phi(\dot{M})$, we will scale from the empirically measured rates for the high-luminosity globular cluster X-ray sources and galactic plane CVs.

As discussed in § II, the luminous X-ray sources form a complete sample of accreting binaries. Thus we may use their distribution of $\dot{M}$ to infer a distribution function for $\dot{M}$. As there is reason to believe that the accretion mechanism is the same in LMXRBs and CVs (Patterson 1984), we assume that the accreting white dwarfs in globular clusters have the same distribution of accretion rates as the accreting neutron stars. The accretion rate for the luminous sources may be directly measured from the X-ray luminosity, since

$$L_x = \frac{\epsilon G m_x \dot{M}}{R_x} . \tag{4}$$

For neutron stars, $m_x \approx 1.4\ M_\odot$ and $R_x \approx 7.0$ km (Rappaport and Joss 1981; Arnett and Bowers 1977), and ϵ, the fraction of the luminosity which emerges as X-rays, is ~ 1.0. Thus the observed luminosity function (Fig. 2) allows a direct estimation of the distribution of accretion rates. We have fitted a power law with slope -1.3 to the bright end of the globular cluster X-ray luminosity function; thus the distribution of accretion rates is

$$\phi(\dot{M})d\dot{M} = k_1 \dot{M}^{-1.3} d\dot{M} . \tag{5}$$

This is consistent with the distribution of $\dot{M}$ for galactic plane CVs (Patterson 1984) where a slope of ~ -1.1 in the distribution of accretion rates is inferred from the optical data. The range of $\dot{M}$ observed in both LMXRBs and CVs is $2 \times 10^{-11}\ M_\odot\ \mathrm{yr}^{-1} < \dot{M} < 3 \times 10^{-8}\ M_\odot\ \mathrm{yr}^{-1}$.

Finally we adopt mass-radius relations so that we may eliminate R_s from equation (2) and R_x from equation (4). The mass-radius relation for globular cluster field stars has been taken to be Patterson's (1984) empirical relationship for lower main-sequence stars,

$$(R_s/R_\odot) = (m_s/M_\odot)^{0.9} . \tag{6}$$

For white dwarfs, we have fitted the Hamada and Salpeter (1961) theoretical calculations, yielding

$$(R_x/R_\odot) = \begin{cases} 0.0078\ (m_x/M_\odot)^{-0.4} , & m_x < 0.7\ M_\odot \\ 0.0040\ (m_x/M_\odot)^{-2.2} , & m_x > 0.7\ M_\odot \end{cases} . \tag{7}$$

Using a simple inverse power-law mass function, i.e., $R_x \propto m_x^{-1}$, also gives similar results in our calculations.

In order to calculate the luminosity function for tidally captured white dwarf binaries in globular clusters, we integrate the probability distribution given in equation (1) with a δ-function which selects out the desired X-ray luminosity, i.e.,

$$\Phi(L_x) = \int dm_s \int dm_x \int d\dot{M} p(m_s, m_x, \dot{M}) \delta[L_x - L(m_x, \dot{M})] , \tag{8}$$

where $L(m_x, \dot{M})$ is given in equation (4) with the compact star being a white dwarf. We have taken ϵ to be ~ 0.03 for accretion onto a white dwarf (cf. Kylafis and Lamb 1982). The assumption that ϵ is independent of $\dot{M}$ is probably not strictly valid. However, given the current lack of understanding of the details of soft X-ray emission in CVs, we have made the simplifying assumption of a constant ϵ.

We have integrated equation (8) using equations (1)–(7) to derive the luminosity function predicted by our model. For the parameters specified above, the total number of low luminosity X-ray sources in an average cluster is

$$N_{\mathrm{tot}} = 9.2 \left(\frac{n_s}{8.3 \times 10^3\ \mathrm{pc}^{-3}} \right) \left(\frac{n_x}{1.3 \times 10^3\ \mathrm{pc}^{-3}} \right) \left(\frac{V}{3.2\ \mathrm{pc}^3} \right) \left(\frac{v_0}{5.7\ \mathrm{km}^{-1}} \right)^{-1.2} \left(\frac{\tau}{10^9\ \mathrm{yr}} \right) , \tag{9}$$

where τ is the X-ray lifetime of the accreting binary. The values of n_s, V, and v_0 are mean values for galactic globular clusters (Madore 1980) and $\tau \approx 10^9$ yr is the time it takes for the secondary to exhaust its mass through accretion (Lightman and Grindlay 1982; Patterson 1984). We have taken $n_x/n_s \approx 0.15$, which is typical for globular cluster mass functions derived to fit surface brightness profiles (Da Costa and Freeman 1976; Illingworth and King 1977). We note that all of the parameter values in equation (9) are uncertain by factors of several, and thus N_{tot} is poorly known. In Figure 3 we present the predicted luminosity function $\Phi(L_x)$, where we have divided the results of integrating equation (8) by N_{tot} to normalize $\Phi(L_x)$ to unit area.

To compare our model with observations, we need to derive the BSLF associated with $\Phi(L_x)$. Consider a globular cluster with $N > 0$ sources and a normalized luminosity function $f(L)$. Let $p_*(L|N)dL$ be the probability that the brightest source (out of N) has a luminosity between L and $L + dL$. A source in the cluster is either less luminous than L, between L and $L + dL$, or more luminous than $L + dL$. The probability that one source is between L and $L + dL$ and zero sources are brighter than $L + dL$ is given by the multinomial distribution

$$p_*(L|N)dL = N f(L)[1 - F(L)]^{N-1} , \tag{10}$$

where

$$F(L) \equiv \int_L^\infty f(L)dL . \tag{11}$$

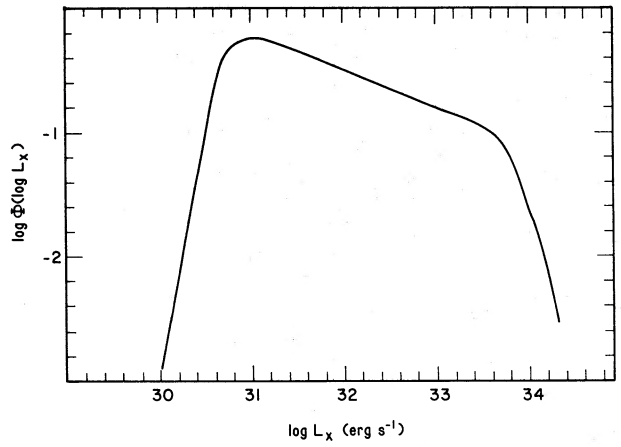

FIG. 3

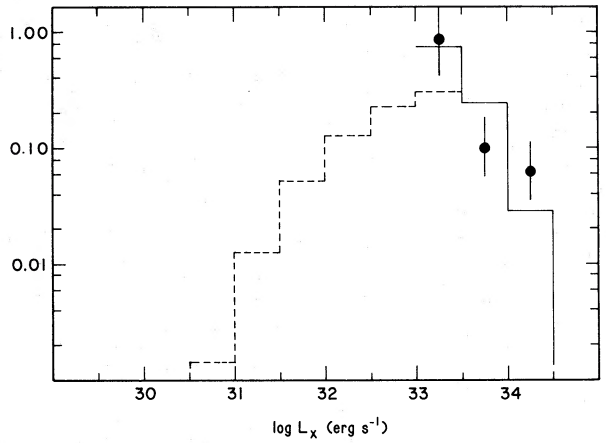

FIG. 4

FIG. 3.—Luminosity function for low-luminosity globular cluster X-ray sources from the simple model described in § V. The model parameters are given in the text. The luminosity function is normalized to have unit area. The ordinate is the logarithm of the 0.5–20 keV X-ray luminosity, and the abscissa is the logarithm of the fraction of sources per decade of luminosity.

FIG. 4.—Brightest source luminosity function (BSLF) derived from the model luminosity function in Fig. 3. The solid line is the model BSLF binned in the same manner as the observed maximum likelihood BSLF shown in Fig. 2, i.e., with the lower bin including all luminosities below 10^{33} ergs s^{-1}. The dashed line shows the model BSLF with all lower luminosity bins resolved. The filled circles are the observational data from the maximum likelihood BSLG in Fig. 2 renormalized to ignore the high-luminosity X-ray sources. The error bars shown are $\pm 1\ \sigma$ Poisson uncertainties based on the number of X-ray sources observed in each luminosity bin.

For $N = 0$, we define $p_*(L|0)dL$ to be 1 for $L = 0$ and 0, otherwise. If λ is the expected number of sources in the cluster, than the probability that there are N is given by the Poisson distribution

$$p(N) = \frac{e^{-\lambda}\lambda^N}{N!} . \tag{12}$$

Finally we have

$$\begin{aligned} p_*(L)dL &= \sum_N p(N)p_*(L|N)dL \\ &= \lambda f(L)e^{-\lambda F(L)}dL . \end{aligned} \tag{13}$$

The probability distribution $p_*(L)$ is normalized and represents the BSLF associated with the normalized luminosity function $f(L)$.

To derive the BSLF associated with our model luminosity function $\Phi(L_x)$, we substitute $f(L) = \Phi(L_x)$ and $\lambda = N_{\rm tot}$ into equation (13). In Figure 4 we have plotted the BSLF derived from the luminosity function in Figure 3 and $N_{\rm tot} = 9.2$. We have also plotted the observed BSLF from Figure 2 and we note that the qualitative agreement is good. Much of the discrepancy is due to the very small number (two or three) of sources in each bin. Thus the uncertainties in the observed maximum likelihood BSLF are considerable.

We have varied the parameters of the model to determine the sensitivity of the BSLF to the input parameters. As noted above, the BSLF is insensitive to the exact form of the input functions. However it is sensitive to two combinations of parameters. One is the maximum possible X-ray luminosity, $L_{\rm max}$. This luminosity is related to the model parameters by the relation

$$L_{\rm max} = \frac{G\epsilon m_{x,\,\rm max}\dot{M}_{\rm max}}{R_x(m_{x,\,\rm max})} . \tag{14}$$

As the maximum white dwarf mass is $\sim 1\ M_\odot$, the maximum X-ray luminosity is

$$L_{\rm max} \approx \epsilon\left(\frac{\dot{M}_{\rm max}}{10^{-8}\ M_\odot\ {\rm yr}^{-1}}\right) 3 \times 10^{35}\ {\rm ergs\ s}^{-1} . \tag{15}$$

The observations require that $L_{\rm max} \geq 3 \times 10^{34}$ ergs s^{-1} since two globular clusters (NGC 104 and NGC 5284) contain sources with approximately that luminosity. Note that the uncertainty introduced into the model by assuming that ϵ is independent of $\dot{M}$ is reflected in the difficulty of deriving ϵ and $\dot{M}_{\rm max}$ from the observed quantity $L_{\rm max}$.

The second combination of parameters which the BSLF is sensitive to is $N_{\rm tot}$. A little thought about equation (13) reveals that the BSLF will peak near the luminosity where $\lambda F(L) \approx 1$. In the context of the model, $\lambda = N_{\rm tot}$ and $F(L)$ is the fraction of sources brighter than L. Figure 3 shows that $\Phi(L_x)$, and hence $F(L_x)$, is a slowly varying function of L_x over most of its range. Thus small changes in $N_{\rm tot}$ result in large changes in the BSLF. Note that the value of $N_{\rm tot}$ which best fits the observed BSLF is dependent on $L_{\rm max}$. An approximate relationship is given by

$$N_{\rm tot} \approx \left(\frac{L_{\rm max}}{10^{35}\ {\rm ergs\ s}^{-1}}\right)^{-2} \tag{16}$$

and was derived empirically by computing and fitting several models to the observed BSLF.

In concluding this section, we reiterate what we believe is the primary result of this exercise. The simple model presented here adequately fits the observed BSLF for reasonable values of the parameters. The calculated BSLF is insensitive to the exact form of the input formulae, e.g., the capture cross section and the mass functions. However, fitting the model to the data constrains L_{max} and N_{tot}. For reasonable values of L_{max}, which can be inferred from the data, the total number of low luminosity X-ray sources in an average globular cluster is ~ 10.

VI. DISCUSSION

The models discussed in the previous section, when fitted to the observed BSLF for normalization, indicate that the number of tidally captured, X-ray active white dwarf binaries is ~ 10 per cluster. This, however, is an average number and N_{tot} depends strongly on the properties of individual globular clusters as well as statistical fluctuations in the number of tidal captures realized. Using equation (19) and tabulated values of globular cluster properties (see § IV), we note that the expected value of N_{tot} varies from <0.1 to >100 for galactic globular clusters. This wide range of possible values implies that the results of § V cannot be applied to single clusters; rather, they are meant to be applied to samples of globular clusters large enough to speak reasonably of a typical globular cluster.

Krolik (1984) and HG have both estimated the number of X-ray active white dwarf binaries in a typical globular cluster. HG estimated ~ 30 by integrating under the BSLF and extrapolating to low luminosities. However, our models are inconsistent with a value this high. If there were ~ 30 low-luminosity X-ray sources in each cluster, the BSLF would peak above $\sim 3 \times 10^{35}$ ergs s^{-1}, in conflict with the observed BSLF. Krolik (1984) modeled the dynamics of binary formation in globular clusters and predicted ~ 1000 CVs in galactic globular clusters, in good agreement with our models. The agreement between Krolik and our work using two different techniques for estimating the number of low-luminosity X-ray binaries in globular clusters lends support to the models used and the numerical results obtained.

There are several implications of our model which should be noted. The distribution of m_t, where m_t is the total mass of an X-ray system (i.e., $m_t = m_s + m_x$), may be calculated by substituting a δ-function of m_t for the δ-function of L_x in equation (8). We have done this calculation; the mean mass of a tidally captured white dwarf binary is $\sim 1.10\ M_\odot$, and 90% of the binaries have masses between 0.85 and 1.35 $M_\odot$. In a relaxed globular cluster, which most clusters containing X-ray sources are because of their short relaxation times (see § IV), more massive systems are likely to be located near the cluster center. The probability that a system of mass m_t can be found at a given projected distance from the cluster center has been calculated by Lightman, Hertz, and Grindlay (1980). The probability depends on the mean mass of stars in the globular cluster, which we take to be $\langle m_s \rangle = 0.32\ M_\odot$ based on the Gunn and Griffin (1979) mass function which we have adopted.

By convolving the distribution of m_t with the probability that a system with mass m_t will be located at a given projected radial offset (scaled to the cluster's core radius) from the cluster center, we can predict a distribution of radial offsets which can be compared with that observed for the low-luminosity globular cluster X-ray sources by HG. Our models indicate that 90% of the sources should lie within the core radius of the cluster and less than 1% will be more than five core radii from the cluster center. HG observed 14 low-luminosity sources in eight globular clusters. Of the eight sources which are the brightest in the each of the eight clusters, six lie within the core radius, in agreement with the model. However, two or three of the six nonbrightest sources lie more than five core radii from the cluster core. The reason for this apparent dichotomy in radial offset is not clear (see Hertz 1984).

If we know the number of CVs in globular clusters, then we can estimate the number of classical novae which should have been observed in globular clusters. The observed fraction of galactic plane CVs which are classical novae is ~ 0.07 (Patterson 1984). For an assumed recurrence time of $\sim 10^4$ yr, we would expect to have seen approximately one historical nova in galactic globular clusters within the last 100 yr. In fact, one to three have been observed (Webbink 1980; Trimble 1980).

We also note that some of the white dwarfs in globular clusters may have been tidally captured more than once. If 10 white dwarfs are captured every 10^9 yr out of a total of 5000 white dwarfs per cluster, then the probability of binary capture is $\sim 2 \times 10^{-12}$ per white dwarf per year. In 10^{10} years, the probability of capture twice is $\sim 4 \times 10^{-4}$ per white dwarf. Thus out of 5000 white dwarfs in each of 100 clusters, perhaps 200 white dwarfs have been tidally captured twice. Of these, $\sim 10\%$ may be X-ray active. These white dwarfs, already having accreted most of the mass from their first stellar companion, may be significantly more massive than a typical white dwarf and may thus have correspondingly higher X-ray luminosities than white dwarfs which have been tidally captured only once. There is some nonnegligible chance that a white dwarf could accrete enough mass in two episodes of accretion from low-mass companions to exceed the Chandrasekhar limit and evolve into a neutron star.

Finally, the gap in the luminosity function for globular cluster X-ray sources can be understood in terms of our model. The lower end of the gap is established by the maximum luminosity of accreting white dwarfs; as discussed in the previous section, this luminosity is determined by $\epsilon \dot{M}_{max}$. The upper end of the gap is the minimum luminosity which neutron stars, accreting from a Roche lobe filling companion, can sustain. Since $\epsilon \approx 1$ for accretion onto a neutron star, this minimum luminosity is set by the minimum accretion rate an evolving close binary can produce. Evolved binaries have low accretion rates which are driven by gravitational radiation (Rappaport, Joss, and Webbink 1982) and have a minimum at $\sim 10^{-11}\ M_\odot$ yr^{-1}. This yields the observed minimum luminosity.

However, the physical phenomena leading to a gap in the luminosity phenomena are not unique to globular clusters. A gap in the luminosity function is expected, and observed, in the galactic plane if CVs and LMXRBs are considered together. The brightest CV observed in the plane has $L_x \approx 5 \times 10^{32}$ ergs s^{-1} (Córdova and Mason 1984), and the least luminous LMXRB has $L_x \approx 5 \times 10^{35}$ ergs s^{-1} (Bradt and McClintock 1983). Thus there is apparently a gap in the galactic plane CV/LMXRB X-ray luminosity luminosity function.

One possible objection to the model we have proposed is that the maximum luminosity observed for low-luminosity globular cluster X-ray sources is significantly higher than the maximum X-ray luminosity observed for galactic plane CVs, which are morphologically similar. In general there is no reason to expect the luminosity function for CVs formed by tidal capture to be the

same as that for CVs which evolved from initial binaries, such as those in the galactic plane (Patterson 1984). However, the maximum luminosity should be regulated by the same physical mechanisms, so perhaps this difference needs to be addressed. There are several effects which may account for the difference in maximum observed luminosity.

The cross section for tidal capture (eq. [2]) is an increasing function of m_x. Thus tidal capture selects higher mass, and therefore higher gravitational potential, white dwarfs from the field population of white dwarfs. We estimate that this effect may account for an $\sim 20\%$ increase in X-ray luminosity among tidally captured white dwarfs. In addition, the process of tidal capture may produce a massive accretion disk which needs to dissipate from the system before steady state accretion can begin (Krolik, Meiksin, and Joss 1984; Krolik 1984). This additional, though temporary, accretion may produce significantly higher X-ray luminosities for selected systems.

The difference between the maximum X-ray luminosity observed in galactic plane CVs and in globular cluster CVs is due primarily to selection effects and observational biases (Hertz 1984). We observed $\gtrsim 1000$ CVs in globular clusters (~ 10 CVs in each of ~ 100 clusters) and discovered about three with luminosities near 10^{34} ergs s^{-1}. These sources are all X-ray selected. Thus perhaps 300 X-ray selected CVs need to be observed to discover a single X-ray luminous CV. Three X-ray surveys which may yield X-ray selected CVs are the *Einstein* Medium Sensitivity Survey (Gioia *et al.* 1984), the *HEAO* A-1 All Sky Survey (Wood *et al.* 1984), and the *Einstein* Galactic Plane Survey (Hertz and Grindlay 1984*a*). The Medium Survey is a survey of serendipitous X-ray sources discovered in high galactic latitude *Einstein* IPC fields; all sources have been optically identified and the single CV discovered has a typical X-ray luminosity (Stocke *et al.* 1983). Assuming standard CV demography (Patterson 1984), about three CVs are located in the volume of space surveyed to 10^{34} ergs s^{-1} by the 90 deg^2 Medium Survey. This is too few to expect discovering a high X-ray luminosity CV by a factor of 100. Approximately 400 CVs are located in the volume of space surveyed by the *HEAO* A-1 instrument. There may be a high X-ray luminosity CV among the ~ 500 unidentified *HEAO* A-1 sources. The large 1H error boxes, the likelihood that the source is at a low galactic latitude, and the expected faintness of the optical counterpart all make it unlikely that this one CV will be identified. The Galactic Plane Survey is a low galactic latitude counterpart to the Medium Survey; optical identification of sources is incomplete at this time (Grindlay and Hertz 1984). A large number (> 500) of CVs may be in the volume of space surveyed, although the exact number is very sensitive to the distribution of CVs in the galactic plane. Although this may be the best sample to search for high X-ray luminosity CVs, the crowded heavily reddened optical fields and the expected faintness ($V > 17$) of any optical counterparts make it difficult to identify these sources.

Only ~ 25 optically selected galactic plane CVs have measured X-ray luminosities (Córdova and Mason 1984). We therefore expect the maximum observed luminosity to be higher for globular cluster CVs since, by virtue of having observed more CVs, we have detected CVs from farther out the high-luminosity tail of the luminosity function. If the luminosity function has a slope of about -1 for both populations, than we would expect the maximum observed luminosity to be ~ 40 times higher for globular cluster CVs than galactic plane CVs, even if the maximum possible luminosity is the same for both populations. This is in reasonable agreement with the data.

Thus the difference in maximum observed luminosity between galactic plane and globular cluster CVs can be completely explained in terms of selection effects and observational biases. Several observational tests of this model may be possible now and in the future. Spectral information on the low-luminosity globular cluster X-ray sources, either from a spectrometer of sufficient sensitivity or from combining broad-band photometry in several energy bands, can test to determine whether the sources have X-ray spectra similar to galactic plane cataclysmic variables. When AXAF is available, several other observational tests are possible. The radial offsets of the sources may be measured and their mass determined statistically, similar to the technique used to determine the mass of the high-luminosity sources (Grindlay *et al.* 1984). This mass may be compared to the mean binary system mass of ~ 1.1 $M_\odot$ predicted by our model. The most compelling test may come, however, through determining the luminosity function to $< 10^{32}$ ergs s^{-1} from observations of many globular clusters. The tidal capture model predicts a turnover in the luminosity function below $\sim 10^{32}$ ergs s^{-1}. In addition, all globular clusters with parameters favorable to the formation of tidally captured binaries are expected to have an X-ray source brighter than $\sim 10^{32}$ ergs s^{-1}.

APPENDIX

TWO-SIDED KOLMOGOROV-SMIRNOV TEST

The Kolmogorov-Smirnov test (see, e.g., von Mises 1964) determines the probability that a distribution of observed values could have been drawn from a particular known distribution. In the two-sided test, the probability that the observed distribution lies within a specified tolerance of the known distribution is tested, whereas the one-sided test examines the chance that the observed distribution lies to one side of the known distribution. In § IV, the observed distribution was the distribution of parameters of globular clusters containing X-ray sources and the known distribution was the distribution of parameters for all globular clusters. If the parameter in which we are interested is x, then $S_n(x)$, the observed discrete (step-function) cumulative distribution, is defined to be the relative frequency of observations with parameter values less than or equal to x out of the total sample of n observations. The two-sided K-S test defines a test statistic $D_n^{\pm}$ in terms of the deviation of the observed distribution from the known distribution,

$$D_n^{\pm} \equiv \operatorname*{Sup}_x \{|S_n(x) - F(x)|\} , \tag{A1}$$

where $F(x)$ is the known cumulative distribution. What is required is a method of determining the probability that $D_n^{\pm}$ exceeds some threshold ϵ. The power of the K-S test lies in the fact that this probability is independent of the form of the known distribution F (Wald and Wolfkowitz 1939). Massey (1950) has solved the problem where $\epsilon = k/n$ and k is integral. We have generalized Massey's

algorithm, which involves counting all of the possible paths by which a particular value of $D_n^{\pm}$ can be obtained, to allow any rational ϵ, i.e., $\epsilon = k/l$, where k and l are integral. The desired probability, $P_n(\epsilon)$, can be calculated as follows. For integers j and h, let

$$\beta \equiv (j + 1 - h)(n/l) , \tag{A2}$$

where n and l are as above; then

$$G_{j,h} = \begin{cases} 1/\beta! , & \text{for } \beta \text{ integral} \\ 0 , & \text{otherwise} . \end{cases} \tag{A3}$$

Define recursively $U_j(m)$ where

$$U_j(0) = \begin{cases} 0 , & j \neq k \\ 1 , & j = k \end{cases} \tag{A4}$$

and

$$U_j(m + 1) = \sum_{h=1}^{j+1} G_{j,h} U_h(m) . \tag{A5}$$

Then the desired probability (which is the probability that the observations could have been drawn from the known distribution) is

$$P_n(\epsilon) = 1 - \frac{n!}{l^n} U_k(l) . \tag{A6}$$

Computationally, it is most efficient to calculate $P_n(\epsilon)$ in the case where l is a multiple of n.

REFERENCES

Aaronson, M., Schommer, R. A., and Olszewski, E. W. 1984, *Ap. J.*, **276**, 221.
Arnett, W. D., and Bowers, R. C. 1977, *Ap. J. Suppl.*, **33**, 415.
Avni, Y., Soltan, A., Tananbaum, H., and Zamorani, G. 1980, *Ap. J.*, **238**, 800.
Bahcall, J. N., and Ostriker, J. P. 1975, *Nature*, **256**, 23.
Bradt, H. V. D., and McClintock, J. E. 1983, *Ann. Rev. Astr. Ap.*, **21**, 13.
Córdova, F. A., and Mason, K. O. 1984, in *Accretion Driven Stellar X-Ray Sources*, ed. W. H. G. Lewin and E. P. J. van den Heuvel (Cambridge: Cambridge University Press), p. 147.
Da Costa, G. S., and Freeman, K. C. 1976, *Ap. J.*, **206**, 128.
Fabian, A. C., Pringle, J. E., and Rees, M. J. 1975, *M.N.R.A.S.*, **172**, 15P.
Forman, W., Jones, C., Cominsky, L., Julien, P., Murray, S., Peters, G., Tananbaum, H., and Giacconi, R. 1978, *Ap. J. Suppl.*, **38**, 357.
Giacconi, R., *et al.* 1979, *Ap. J.*, **230**, 540.
Gioia, I. M., Maccacaro, T., Schild, R. E., Stocke, J. T., Liebert, J. W., Danziger, I. J., Kunth, D., and Lub, J. 1984, *Ap. J.*, **283**, 495.
Gorenstein, P. 1975, *Ap. J.*, **198**, 95.
Grindlay, J. E., and Hertz, P. 1981, *Ap. J.* (*Letters*), **247**, L17.
———. 1984, *Bull. AAS*, **15**, 1004.
Grindlay, J. E., Hertz, P., Steiner, J. E., Murray, S. S., and Lightman, A. P. 1984, *Ap. J.* (*Letters*), **282**, L16.
Gunn, J. E., and Griffin, R. F. 1979, *A.J.*, **84**, 752.
Hamada, T., and Salpeter, E. E. 1961, *Ap. J.*, **134**, 683.
Hartwick, F. D. A., Cowley, A. P. and Grindlay, J. E. 1982, *Ap. J.* (*Letters*), **254**, L11.
Hays, W. L. 1973, *Statistics* (New York: Holt, Rinehart, and Winston), p. 788.
Hertz, P. 1984, in *Proceedings of the X-Ray Astronomy '84 Symposium, Bologna, Italy*, ed. Y. Tanaka (Institute of Space and Astronautical Science: Tokyo), in press.
Hertz, P., and Grindlay, J. E. 1983*a*, *Ap. J.* (*Letters*), **267**, L83.
———. 1983*b*, *Ap. J.*, **275**, 105 (HG).
———. 1984*a*, *Ap. J.*, **278**, 137.
———. 1984*b*, *Ap. J.*, **282**, 118.
———. 1984*c*, *Ap. J.*, submitted.
Huchra, J. P., and Aaronson, M. 1980, private communication.
Illingworth, G., and King, I. R. 1977, *Ap. J.* (*Letters*), **218**, L109.
King, I. R. 1966, *A.J.*, **71**, 64.
Kleinmann, D. E., Klienmann, S. G., and Wright, E. L. 1976, *Ap. J.* (*Letters*), **210**, L83.
Koester, D., and Weidemann, V. 1980, *Astr. Ap.*, **81**, 145.
Krolik, J. H. 1984, *Ap. J.*, **282**, 452.
Krolik, J. H., Meiksin, A., and Joss, P. C. 1984, *Ap. J.*, **282**, 466.
Kukarkin, B. V. 1974, *The Globular Star Clusters* (Moscow: Nauka Publishing House).
Kylafis, N. D., and Lamb, D. Q. 1979, *Ap. J.* (*Letters*), **228**, L105.
———. 1982, *Ap. J. Suppl.*, **48**, 239.
Lewin, W. H. G., and Joss, P. C. 1984, in *Accretion Driven Stellar X-Ray Sources* ed. W. H. G. Lewin and E. P. J. van den Heuvel (Cambridge: Cambridge University Press), p. 41.
Lightman, A. P., and Grindlay, J. E. 1982, *Ap. J.*, **262**, 145.
Lightman, A. P., Hertz, P., and Grindlay, J. E. 1980, *Ap. J.*, **241**, 367.
Liller, W. 1977, *Ap. J.* (*Letters*), **213**, L21.
Lightman, A. P., and Shapiro, S. L. 1978, *Rev. Mod. Phys.*, **50**, 437.
Longmore, A. J., and Hawarden, T. G. 1980, private communication referenced by Malkan, Kleinmann, and Apt (1980).
Madore, B. F. 1980, in *Globular Clusters*, ed. D. Hanes and B. Madore (Cambridge: Cambridge University Press), p. 21.
Malkan, M., Kleinmann, D. E., and Apt, J. 1980, *Ap. J.*, **237**, 432.
Marshall, H. L. 1982, private communication.
Massey, F. J., Jr. 1950, *Ann. Math. Stat.*, **21**, 116.
McClintock, J. E., and Rappaport, S. A. 1984, in *Cataclysmic Variables and Low Mass X-Ray Binaries*, ed. D. Q. Lamb and J. Patterson (Dordrecht: Reidel), in press.
Paczyński, B., and Sienkiewicz, R. 1981, *Ap. J.* (*Letters*), **241**, L27.
Patterson, J. 1984, *Ap. J. Suppl.*, **54**, 443.
Press, W. H., and Teukolsky, S. A. 1977, *Ap. J.*, **213**, 183.
Rappaport, S., and Joss, P. C. 1981, in *X-Ray Astronomy with the Einstein Satellite*, ed. R. Giacconi (Dordrecht: Reidel), p. 123.
Rappaport, S., Joss, P. C., and Webbink, R. F. 1982, *Ap. J.*, **254**, 616.
Rappaport, S., Verbunt, F., and Joss, P. C. 1983, *Ap. J.*, **275**, 713.
Silk, J., and Arons, J. 1975, *Ap. J.* (*Letters*), **200**, L131.
Stocke, J., Liebert, J., Gioia, I. M., Griffiths, R. E., Maccacaro, T., Danziger, I. J., Kunth, D., and Lub, J. 1983, *Ap. J.*, **273**, 458.
Trimble, V. L. 1980, in *IAU Symposium 85, Star Clusters*, ed. J. E. Hesser (Dordrecht: Reidel), p. 259.
Ulmer, M. P., Murray, S. S., Gursky, H., and Bahcall, J. N. 1976, *Ap. J.*, **208**, 47.
von Mises, R. 1964, *Mathematical Theory of Probability and Statistics* (New York: Academic Press).
Wald, A., and Wolfkowitz, J. 1939, *Ann. Math. Stat.*, **10**, 105.
Webbink, R. F. 1980, in *IAU Symposium 88, Close Binary Stars: Observations and Interpretation*, ed. M. J. Plavec, D. M. Popper, and R. K. Ulrich (Dordrecht: Reidel), p. 398.
Webbink, R. F., Rappaport, S., and Savonije, G. J. 1983, *Ap. J.*, **270**, 678.
Wood, K. S., *et al.* 1984, *Ap. J. Suppl.*, **56**, 507.
Zombeck, M. V. 1982, *Handbook of Space Astronomy and Astrophysics* (New York: Cambridge University Press).

PAUL HERTZ and KENT S. WOOD: Code 4121, Naval Research Laboratory, Washington, DC 20375